17th World Conference on Earthquake Engineering, 17WCEE

Sendai, Japan - September 13th to 18th 2020

INFLUENCE OF NONLINEARITY OF FLANGE JOINT ON SEISMIC RESPONSE OF PORCELAIN PILLAR ELECTRIACAL EQUIPMENT

Y D. Xue(1), Y F Cheng(2), Z B Zhu(3),S Li(4), Z L Liu(5),H L Guo(6), S J.Zhang(7)

(1) Beijing, China, China Electric Power Research Institute, xuecumtb@163.com

(2) Beijing, China, China Electric Power Research Institute, cyf@ epri.sgcc.com.cn

(3) Beijing, China, China Electric Power Research Institute, zhuzb@ epri.sgcc.com.cn

(4)Beijing, China, China Electric Power Research Institute, lisheng@epri.sgcc.com.cn

(5) Beijing, China, China Electric Power Research Institute, liuzhenlin@epri.sgcc.com.cn

(6) Tianjin, China, Tianjin University, hlguo@tju.edu.cn

(7)Hangzhou, China, State Grid Zhejiang Electric Power Co., Ltd,bluemoon_789@126.com

Abstract

The pillar insulator is an important component in the substation. The seismic damage data indicates that the pillar electrical equipment is more vulnerable under earthquake, and the root of the equipment and the flanged joint are weak links. The bending stiffness of the flange joint is mostly based on the elastic theory. Under the large earthquake excitation, the uncoordinated deformation at the flange joint will make the structure exhibit nonlinear characteristics. In order to consider the influence of nonlinear characteristics on the dynamic response of porcelain pillar electrical equipment under seismic excitation, the nonlinear coefficient η which characterizes the flange joint is defined, and the electrical power of 110kV post insulator considering the nonlinear characteristics of the flange connection of the equipment is established. Shaking table test is conducted. The theoretical analysis results have a good fit with the experimental results, verifying the correctness of the dynamic model, and revealing the nonlinear seismic response law of the porcelain pillar equipment. The results show that the nonlinear calculation results of the top displacement of the porcelain pillar and the stress at the bottom end of the porcelain pillar are smaller than the linear calculation results. With the increase of the seismic excitation, the difference between the two increases gradually, and the nonlinear characteristics are more obvious. When the seismic excitation is 0.5g, the displacement and stress difference are 2% and 17.4% respectively. Under the excitation of each seismic wave, when the nonlinear stiffness coefficient changes within 0-10^5, the maximum stress at the bottom end of the porcelain pillar is divided into three stages: basically no change, steady decline, and rapid decline. With the nonlinear stiffness $\eta=2\times10^4$, when the seismic excitation is 0.2g, 0.3g, 0.4g, 0.5g, the maximum stress at the bottom end of the porcelain pillar is reduced by 5%, 9.5%, 13%, 17%, respectively ; With the nonlinear stiffness $\eta=4\times10^4$, when the seismic excitation is 0.2g, 0.3g, 0.4g, 0.5g, the maximum stress at the bottom end of the porcelain pillar is 8.7%, 14.3%, 19%, 24%, respectively. The research conclusions can provide a theoretical reference for the pillar electrical equipment.

Keywords: Nonlinear, Porcelain pillar, Flange connection, Seismic response, Maximum stress

1.Introduction

China is located between the circum-Pacific seismic belt and the Eurasian seismic belt. The previous earthquakes have damaged China's electrical equipment seriously, especially the porcelain pillar electrical equipment in substations, which has affected the safe and stable operation of the power grid and caused huge economic losses. In the earthquake, the root fracture of porcelain bushing is very easy to occur in the electrical equipment with porcelain pillar insulation, such as arrester, current transformer, voltage transformer, circuit breaker, etc. The main reasons for this situation are as follows: due to the structural characteristics and material properties of the equipment, the natural frequency of this kind of electrical equipment is generally between 1-10 Hz, which is close to the excellent frequency of the earthquake. Under the earthquake excitation, the equipment is prone to resonance; because of the brittleness and weak energy storage of ceramic materials, the bending resistance of ceramic casing is poor, and the large deformation caused by resonance, the root of ceramic pillar should be The force exceeds the strength of the ceramic, resulting in the fracture of the root of the ceramic sleeve.

At present, many researches have been done on the calculation of flange connection stiffness and the simplification of the model. Li S et al. [1] have established the mechanical model of the porcelain pillar equipment based on the gluing characteristics of the flange joint, studied its dynamic characteristics, and proposed the bending stiffness calculation formula considering the gluing characteristics. Paolacci [2] has carried out the seismic analysis of the porcelain pillar circuit breaker by establishing the 3D solid finite element model in the analysis, the equivalent beam element is used to replace the flange joint; Zhang et al. [3] obtained the stiffness coefficient of the porcelain strut and flange connection of the UHV Transformer; In reference [4-5], the rotation response between the porcelain bushing and the metal flange was studied by shaking table test. It was found that the excessive inclination of the joint would lead to the failure of the bushing during the earthquake. Japanese code [6] and Chinese code [7] have given the calculation formula of flange joint stiffness, but the calculation formula is mostly for the voltage level below 500kV, and the applicability of the calculation formula for higher voltage level needs further study.

However, all of the above studies are based on the elastic range to consider the connection between the porcelain column casings and calculate the stiffness. In application, the deformation of the equipment is discontinuous due to the different materials of the gluing part, and there is a nonlinear response. In this paper, the nonlinear stiffness is introduced to establish the dynamic model of 110kV post insulator electrical equipment considering the nonlinear characteristics of the equipment flange joint, and the shaking table test is carried out to prove the correctness of the nonlinear dynamic model, revealing the non-linear seismic response law of the porcelain post equipment.

2. Dynamic Model of Porcelain Pillar Equipment Considering the Nonlinearity of Flange Connection

In this section, the non-linear dynamic model research is carried out for the porcelain pillar electrical equipment with bracket, and the 110kV porcelain pillar equipment with bracket is taken as the research object, as shown in Fig. 1. The porcelain pillar is connected with the steel frame through the flange, and the bracket is fixedly connected with the ground. Set the angle of the top of the bracket as θ0, and the angle of the porcelain pillar as θ1 when the equipment is subjected to seismic excitation.

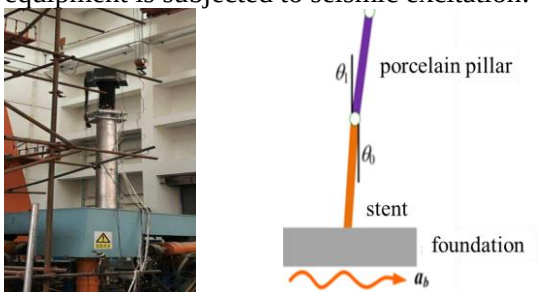

Fig.1−Calculation model diagram

2.1 Dynamic model of porcelain pillar equipment

If the stiffness of the flange at the bottom of the upper porcelain pillar is kid and that at the top of the lower porcelain pillar is k(i-1)u, the equivalent stiffness at the flange joint can be expressed as:

$$k_i = \frac{k_{id} k_{(i-1)u}}{k_{id} + k_{(i-1)u}} \tag{1}$$

Where, k_{id}, $k_{(i-1)u}$ is calculated as follows:

$$\begin{aligned} k_{id} &= \beta_d d_d h_d^2 / t_d \\ k_{iu} &= \beta_u d_u h_u^2 / t_u \end{aligned} \tag{2}$$

Among them, d_u and d_d are the outer diameter of the upper and lower flange and porcelain sleeve gluing position, h_u and h_d are the height of the upper and lower flange and porcelain sleeve gluing position, t_u and t_d are the gap distance between the upper and lower flange and porcelain sleeve, β_u and β_d are the bending rigidity coefficient of the upper and lower flange and porcelain sleeve connection position; when the outer diameter of porcelain sleeve tube at the gluing position is less than 275mm, 6.54×10^7 is taken, and when the outer diameter of porcelain sleeve at the gluing position is greater than 375mm, 5.0×10^7 is taken. When the outer diameter of the porcelain bushing in the glued part is between 275mm and 375mm, it can be obtained by linear interpolation.

It can be seen from the above analysis that the rotation moment caused by the relative rotation of the upper and lower flange plates is:

$$M_i=k_i(\theta_i-\theta_{i-1}) \tag{3}$$

The above formula is the rotational moment in ideal state. Due to the different materials of flanged joint and the existence of hole gap in the joint, M_i needs to include non-linear items considering these factors, so as to be more in line with the actual situation. After considering nonlinear factors, equation (3) is written as:

$$M_i=k_i[(\theta_i-\theta_{i-1}) +\eta(\theta_i-\theta_{i-1})^3] \tag{4}$$

If there are Nc porcelain pillars, there are Nc flanged joints. The total elastic potential energy at the flanged joints is:

$$U_k = \frac{1}{2}k_1\theta_1^2 + \frac{1}{4}\eta k_1\theta_1^4 + \sum_{i=2}^{N_c}\left[\frac{1}{2}k_i\left(\theta_i-\theta_{i-1}\right)^2 + \frac{1}{4}\eta k_i\left(\theta_i-\theta_{i-1}\right)^4\right] \tag{5}$$

Due to the change of gravity potential energy of porcelain pillar caused by rotation of porcelain pillar, the total gravity potential energy is as follows:

$$U_g = -\frac{1}{2}\sum_{i=1}^{Nc} m_i g\left(\sum_{j=1}^{i} L_j\theta_j^2 - \frac{1}{2}L_i\theta_i^2\right) \tag{6}$$

Kinetic energy of porcelain pillar includes translational kinetic energy and rotational kinetic energy, specifically:

$$T = \frac{1}{2}\sum_{i=1}^{N_c} m_i v_{c,i}^2 + \frac{1}{2}\sum_{i=1}^{N_c}\frac{1}{12}m_i L_i^2\dot{\theta}_i^2 \tag{7}$$

Where $v_{c,i}$ is the centroid velocity of section i of the porcelain pillar, and the velocity relationship of section i of the porcelain pillar is shown in Fig. 3.

For steel support, the elastic potential energy of the support is:

$$U_z = \frac{1}{2}\int_0^{L_0} EI\left(\frac{\partial^2 y}{\partial x^2}\right)^2 \mathrm{d}x \tag{8}$$

The total potential energy of the stent and porcelain pillar system is:

$$U = U_k + U_g + U_z \tag{9}$$

The kinetic energy of the stent is:

$$T_z = \frac{1}{2}\int_0^{L_0} \rho_z A_z \left(\frac{\partial y}{\partial t} + \frac{dy_b}{dt}\right)^2 \mathrm{d}x \tag{10}$$

y_b is the ground displacement.

As an example of the flange connected porcelain strut and the stent connecting equipment, the kinematic analysis of the upper end strut of the stent is shown in Fig. 3.

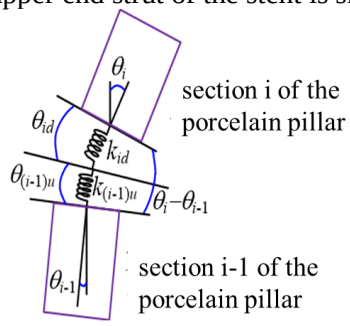

Fig. 2-Calculation model of flanged joint

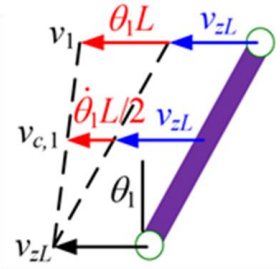

Fig. 3-Kinematic analysis of porcelain pillar

For the electrical equipment with single porcelain pillar, the centroid velocity of the porcelain pillar is:

$$v_{c,1} = v_{zL} + \frac{1}{2} L_1 \dot{\theta}_1 \tag{11}$$

Where v_{zL} is the horizontal velocity at the top of the stent, which can be expressed as follows:

$$v_{zL} = \dot{y}(L_0, t) + \dot{y}_b \tag{12}$$

Substituting Hamilton variational equation:

$$\int_{t_1}^{t_2} (\delta T - \delta U)\mathrm{d}t = 0 \tag{13}$$

The dynamic equation of the system can be obtained.

2.2 Dynamic Equation of Porcelain Pillar Equipment

Taking 110kV porcelain pillar equipment with stent as an example, the nonlinear dynamic equation of the system is obtained by Hamilton variational principle. In this paper, Galerkin was used to discretize the model of ceramic props with supports, and make y=Y(x)q(t), Y(x) is the modal function of the supports. Since the bottom end of the stent is fixed, the top end is connected with the porcelain pillar equipment. In this case, the boundary conditions are:

$$\begin{aligned} &y(0,t) = 0 \qquad \frac{\partial y(0,t)}{\partial x} = 0 \\ &\frac{\partial y(l,t)}{\partial x} = \theta_0 \quad EI\frac{\partial^2 y(l,t)}{\partial x^2} = k_1(\theta_1 - \theta_0) \end{aligned} \tag{14}$$

In the following, Galerkin method is used to discretize the dynamic equation (14) of the supported system, Let y=φ(x)q(t), where φ(x) is the modal equation of the beam. By substituting y=φ(x)q(t) and modal equation of beam φ(x)= $C_1\cos\beta x+C_2\mathrm{S}\sin\beta x+C_3\cosh\beta x+C_4\sinh\beta x$ into equation (14), we can get

$$\begin{aligned} &C_1 + C_3 = 0, C_2 + C_4 = 0 \\ &\beta\left(-C_1\sin\beta l + C_2\cos\beta l + C_3\sinh\beta l + C_4\cosh\beta l\right)q(t) = \theta_0 \\ &EI\beta^2\left(-C_1\cos\beta l - C_2\sin\beta l + C_3\cosh\beta l + C_4\sinh\beta l\right)q(t) = k_1(\theta_1 - \theta_0) \end{aligned} \tag{15}$$

The change of kinetic energy is divided into:

$$-\delta T=m_1\left(\alpha\ddot{\theta}_0+\ddot{y}_b+\frac{1}{2}L_1\ddot{\theta}_1\right)\left(\alpha\delta\theta_0+\frac{1}{2}L_1\delta\theta_1\right)+\frac{1}{12}m_1L_1^2\ddot{\theta}_1\delta\theta_1 \quad (16)$$
$$+\frac{\rho_z A_z}{Y'^2(L_0)}\int_0^{L_0}Y^2(x)\mathrm{d}x\ddot{\theta}_0\delta\theta_0+\frac{\rho_z A_z}{Y'(L_0)}\int_0^{L_0}Y(x)\mathrm{d}x\ddot{y}_b\delta\theta_0$$

The change of potential energy can be divided into:

$$\delta U=k_1(\theta_1-\theta_0)(\delta\theta_1-\delta\theta_0)+\eta_1(\theta_1-\theta_0)^3(\delta\theta_1-\delta\theta_0)-\frac{1}{2}m_1gL_1\theta_1\delta\theta \quad (17)$$
$$+\frac{E_zI_z}{Y'^2(L_0)}\int_0^{L_0}\frac{d^4Y(x)}{dx^4}Y(x)\mathrm{d}x\theta_0\delta\theta_0$$

By substituting the Hamilton variational equation, the following results are obtained:

$$\left(m_0+\alpha^2m_1\right)\ddot{\theta}_0+\frac{1}{2}m_1\alpha L_1\ddot{\theta}_1+k_0\theta_0-k_1(\theta_1-\theta_0)-\eta_1(\theta_1-\theta_0)^3=-\left(F_0+\alpha m_1\right)\ddot{y}_b \quad (18)$$

$$\frac{1}{2}m_1\alpha L_1\ddot{\theta}_0+\frac{1}{3}m_1L_1^2\ddot{\theta}_1-\frac{1}{2}m_1gL_1\theta_1+k_1(\theta_1-\theta_0)+\eta_1(\theta_1-\theta_0)^3=-\frac{1}{2}m_1L_1\ddot{y}_b \quad (19)$$

Where $\ddot{y}_b=fa_b$, $m_0=\frac{\rho_z A_z}{Y'^2(L_0)}\int_0^{L_0}Y^2(x)\mathrm{d}x$, $k_0=\frac{E_zI_z}{Y'^2(L_0)}\int_0^{L_0}\frac{d^4Y(x)}{dx^4}Y(x)\mathrm{d}x$, $F_0=\frac{\rho_z A_z}{Y'(L_0)}\int_0^{L_0}Y(x)\mathrm{d}x$.

3 Nonlinear Dynamic Response of Electrical Equipment with Porcelain Pillars

3.1 Input of the ground motion

The seismic wave data adopts artificial wave, which is obtained by fitting the seismic acceleration response spectrum with a characteristic period of 0.9s. It is suitable for the seismic design, test and seismic performance evaluation of high-voltage and ultra-high voltage electrical equipment. The artificial wave time history when the seismic acceleration peak value is 1g is shown in Fig. 4.

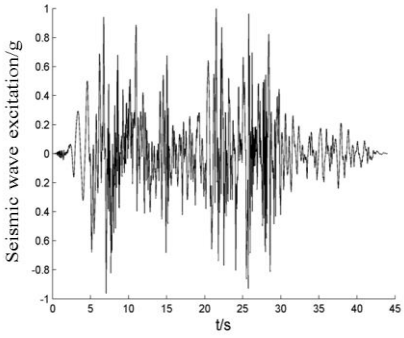

Fig. 4−Time history curve of artificial earthquake

3.2Seismic response of 110 kV post insulator with stent

The theoretical method is used to solve equations (18) and (19) for 110 kV post insulator equipment with stent, and the response of the equipment under different earthquake excitation is obtained. In the nonlinear dynamic equation, when the nonlinear stiffness coefficient η=0, the analysis result is the seismic response of the equipment in the elastic state; when η≠0, it is the seismic response of the equipment in the nonlinear state. The η value is difficult to be solved by theoretical calculation. In this study, the method of comparison with the test results is used to obtain the value of η, that is, in the analysis program, the η value changes within a certain range, and the difference between the theoretical analysis result and the test result is the smallest, then the value of η is taken as the value under this working condition. The comparison of theoretical and experimental results will be verified in Section 4. For 110kV post insulator equipment with

stent, the nonlinear stiffness coefficient η is taken as 20000 after preliminary comparative analysis when considering the nonlinear characteristics.

3.2.1 Seismic response of post insulator without considering nonlinear characteristics

Considering the nonlinear factors of 110kV pillar insulator equipment with stent, that is, the nonlinear stiffness coefficient η of flanged joint is taken as 20000, and the nonlinear seismic response of the equipment under different seismic excitation is analyzed. Fig. 11, 13 and 15 show the top displacement time history curve of 110kV post insulator equipment with bracket when the seismic wave excitation intensity is 0.1g, 0.3g and 0.5g respectively, and Fig. 12, 14 and 16 show the bottom stress time history curve of equipment when the seismic wave excitation intensity is 0.1g, 0.3g and 0.5g respectively.

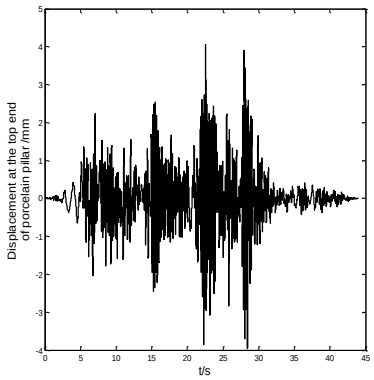

Fig.5−Displacement at the top end of porcelain pillar (f= 0.1g)

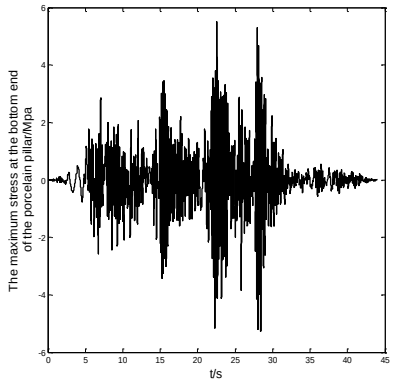

Fig.6−The maximum stress at the bottom end of the porcelain pillar(f= 0.1g)

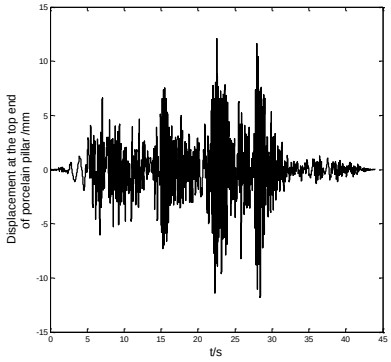

Fig.7−Displacement at the top end of porcelain pillar (f= 0.3g)

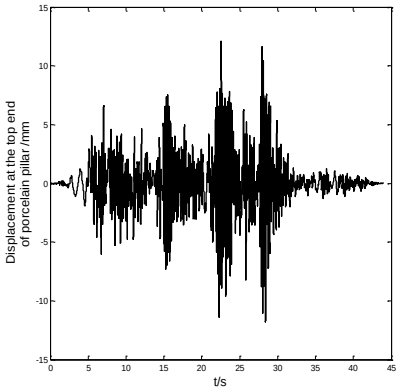

Fig.8−The maximum stress at the bottom end of the porcelain pillar(f= 0.3g)

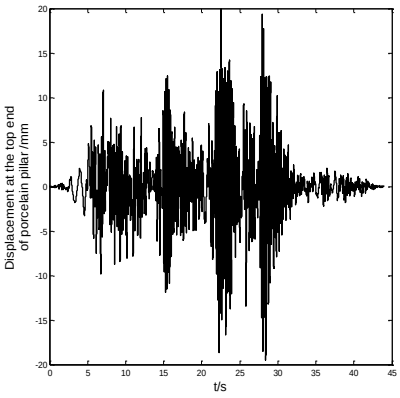

Fig.9−Displacement at the top end of porcelain pillar (f= 0.5g)

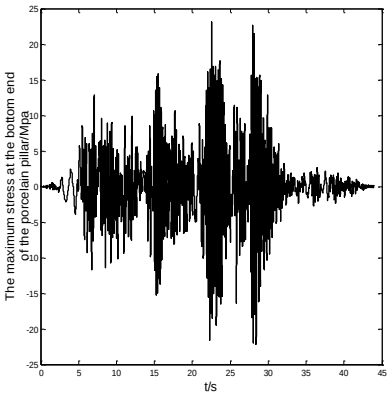

Fig.10−The maximum stress at the bottom end of the porcelain pillar(f= 0.5g)

Combined with the analysis results and the data in the Fig., it can be seen that the seismic response of the equipment, such as displacement and stress, increases nonlinearly with the increase of seismic excitation. When the seismic excitation increases from 0.1g to 0.5g, the displacement response of the equipment increases from 4.1 to 19.9 mm nonlinearly, and the stress response increases from 5.49Mpa to 23.1Mpa nonlinearly.

3.2.2 Seismic response of post insulator considering nonlinear characteristics

Considering the nonlinear factors of 110kV pillar insulator equipment with stent, that is, the nonlinear stiffness coefficient η of flanged joint is taken as 20000, and the nonlinear seismic response of the equipment under different seismic excitation is analyzed. Fig. 11, 13 and 15 show the top displacement time history

curve of 110kV post insulator equipment with bracket when the seismic wave excitation intensity is 0.1g, 0.3g and 0.5g respectively, and Fig. 12, 14 and 16 show the bottom stress time history curve of equipment when the seismic wave excitation intensity is 0.1g, 0.3g and 0.5g respectively.

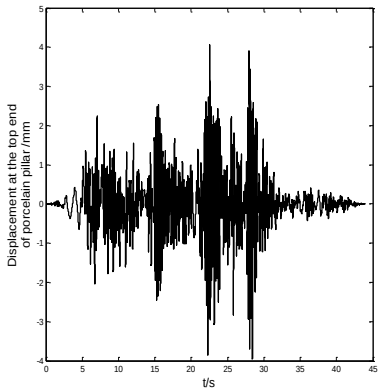

Fig.11−Displacement at the top end of porcelain pillar (f= 0.1g)

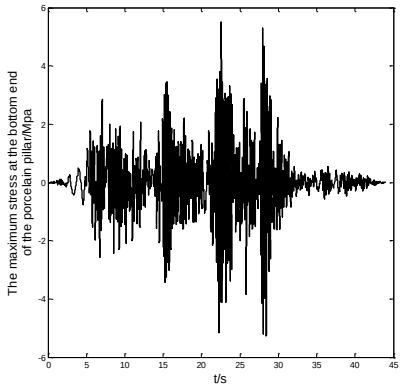

Fig.12−The maximum stress at the bottom end of the porcelain pillar(f= 0.1g)

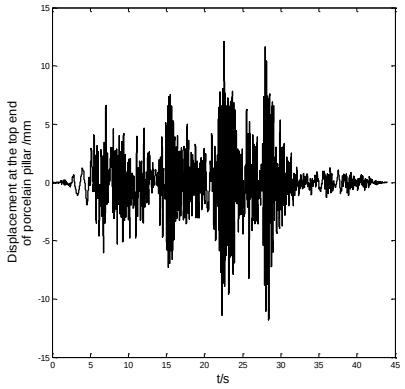

Fig.13−Displacement at the top end of porcelain pillar (f= 0.3g)

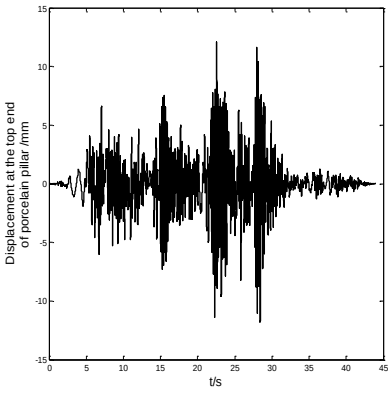

Fig.14−The maximum stress at the bottom end of the porcelain pillar(f= 0.3g)

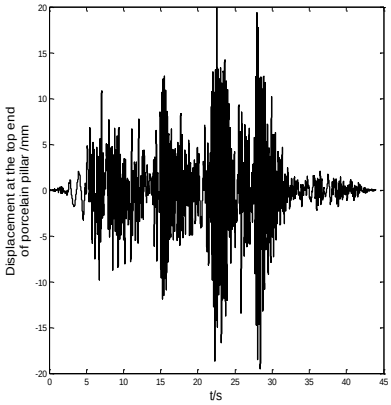

Fig15−Displacement at the top end of porcelain pillar (f= 0.5g)

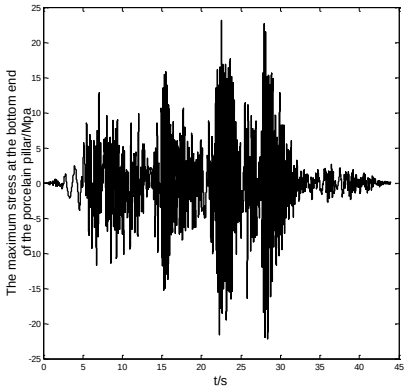

Fig.16−The maximum stress at the bottom end of the porcelain pillar(f= 0.5g)

Combined with the analysis results and the data in the Fig., it can be seen that the seismic response of the equipment, such as displacement and stress, increases nonlinearly with the increase of seismic excitation. When the seismic excitation increases from 0.1g to 0.5g, the displacement response of the equipment increases from 4.1 to 19.9mm nonlinearly, and the stress response increases from 5.49Mpa to 23.1Mpa nonlinearly.

3.2.3 Nonlinear seismic response analysis of 110 kV post insulator equipment with stent

Table 1 shows the maximum displacement response analysis of the equipment under different seismic excitations in case of linearity and considering nonlinearity, and table 2 shows the maximum stress response analysis of the equipment in case of linearity and considering nonlinearity. Fig. 17 and Fig. 18 show the relationship curves between the peak value of different seismic excitation and the maximum displacement response and the maximum stress response, respectively.

Table1-Linear and nonlinear maximum displacement response of equipment under different seismic excitation

Seismic excitation（g）	Maximum displacement（mm）		Difference value	
	Linear	Nonlinear	Numerical difference（mm）	Relative linear percentage（%）
0.1	4.1	4.1	0	0
0.2	8.1	8.1	0	0
0.3	12.2	12.1	0.1	0.83
0.4	16.3	16.0	0.3	1.8
0.5	20.3	19.9	0.4	2.0

Table 2-Linear and nonlinear maximum stress response of equipment under different seismic excitation

Seismic excitation（g）	Maximum stress（Mpa）		Difference value	
	Linear	Nonlinear	Numerical difference（Mpa）	Relative linear percentage（%）
0.1	5.55	5.49	0.06	1.08
0.2	11.16	10.6	0.56	5
0.3	16.73	15.17	1.56	9.3
0.4	22.35	19.37	2.98	13.33
0.5	27.95	23.1	4.85	17.4

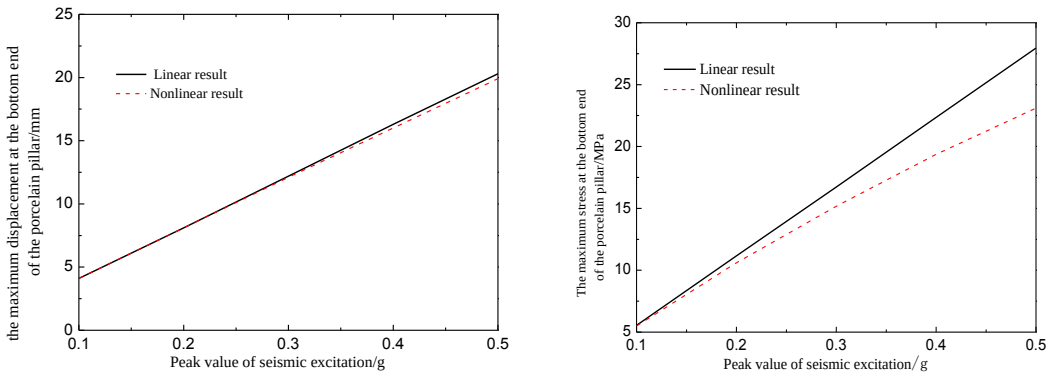

(a)displacement （b）stress

Fig. 18−Relation curve between peak value of different seismic excitation and maximum response of equipment

From the analysis results in the above chart, it can be seen that for 110kV post insulator equipment with bracket, the nonlinear seismic response of the equipment under seismic action is slightly less than the linear seismic response due to the consideration of nonlinear factors. When the earthquake excitation is small, the difference between the linear results and the results considering the nonlinear characteristics is very small. The larger the ground motion excitation is, the larger the difference between the nonlinear response results and the linear response results of the equipment is, the more obvious the nonlinear characteristics are. When the peak value of local vibration acceleration is 0.1g, 0.2g, 0.3g, 0.4g and 0.5g, the difference percentage between the displacement nonlinear analysis result and the linear analysis result is 0%, 0%, 0.83%, 1.8% and 2% respectively, and the difference percentage between the stress nonlinear analysis result and the linear analysis result is 1.08%, 5%, 9.3%, 13.33% and 17.4% respectively. From the above analysis, it can be seen that when the flange connection non-linear is considered The influence on the maximum stress at the bottom of the porcelain pillar is greater than that on the displacement.

3.2.4 Study on the nonlinear seismic response characteristic in the domain of structural parameters

Fig. 19 shows the influence curve of the nonlinear stiffness coefficient on the maximum stress peak value at the bottom of the porcelain pillar in a certain range when the seismic wave excitation is 0.1g, 0.2g, 0.3g, 0.4g and 0.5g. Table 3 shows the maximum stress value at the bottom of the porcelain pillar corresponding to the change of nonlinear stiffness η under different seismic excitation.

It can be seen from Fig. 19 that under different seismic excitations, the influence curve of nonlinear stiffness on porcelain post insulator of 110kV porcelain post insulator equipment with bracket can be divided into three stages: basically no change, steady decline, and rapid decline. It can be seen from table 3 that when the non-linear stiffness changes within the range of 10^0-10^2, the maximum stress at the bottom of the porcelain pillar will not be affected basically; when the non-linear stiffness changes within the range of 102-104, the maximum stress at the bottom of the porcelain pillar will decrease steadily under different earthquake excitation, with the percentage of decrease being 1%, 2.9%, 5.56%, 8.65% and 11.18% respectively; When the nonlinear stiffness changes in the range of 104-105, the decrease of the maximum stress at the bottom of the porcelain pillar increases, and the decrease rate increases. The decrease percentages are 5.9%, 5.93%, 22.65%, 27.79%, 33.43% respectively. From the above analysis, it can be concluded that the larger the seismic wave excitation is, the greater the influence of the nonlinear stiffness on the maximum stress at the bottom of the porcelain pillar is; after considering the nonlinear influence, the larger the seismic excitation is, the greater the decrease of the maximum stress at the bottom of the porcelain pillar is in the rapid decline stage.

Since the parameter η is 20000 after considering the nonlinear characteristics, in order to consider the influence of η on the maximum stress at the bottom of the porcelain pillar when it floats up and down in 20000, this paper analyzes the maximum stress at the bottom of the porcelain pillar when η is [100,4×10^4]. When the seismic wave excitation is 0.1g, 0.2g, 0.3g, 0.4g, 0.5g, η increases from 0 to 2×10^4, the maximum stress at the bottom of porcelain pillar decreases by 1.4%, 4.9%, 9.5%, 13.2%, 17.3% respectively; when η increases from 2×10^4 to 4×10^4, the maximum stress at the bottom of porcelain pillar decreases by 1.2%, 4.0%, 5.3%, 6.6%, 8.2% respectively. It can be seen from the above analysis that when η changes in the range of [2×10^4, 4×10^4], the maximum stress reduction at the bottom of the porcelain pillar is less than when η changes in the range of [10^0, 2×10^4].

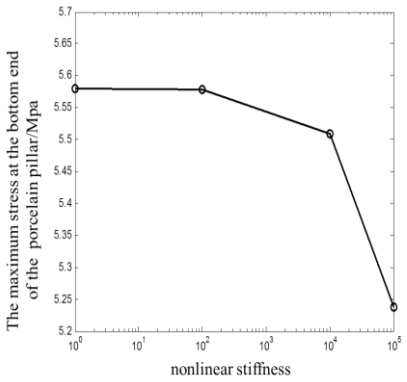

(a)0.1g

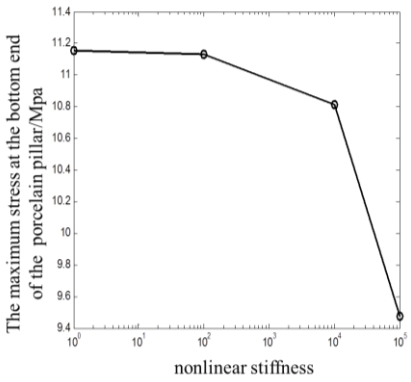

(b)0.2g

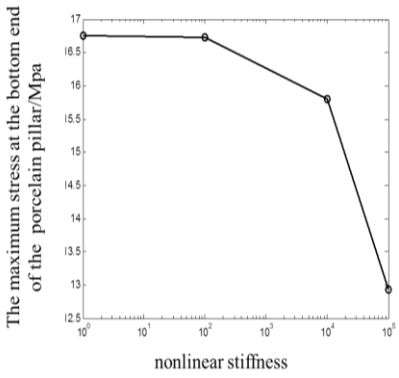

(c)0.3g

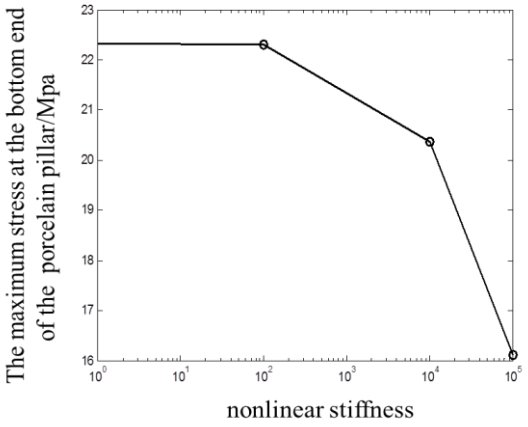

(d)0.4g

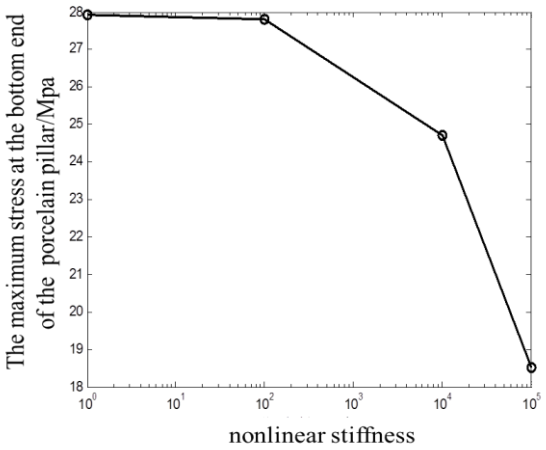

(e)0.5g

Fig. 19–Relation curve between nonlinear stiffness coefficient and maximum stress of equipment under different earthquake excitation

Table 3-The maximum stress value at the bottom of the porcelain pillar with the change of nonlinear stiffness under different earthquake excitation

Earthquake excitation	**The maximum stress at the bottom end of the porcelain pillar/（MPa）**					
	$\eta=10^0$	$\eta=10^2$	$\eta=10^4$	$\eta=2\times10^4$	$\eta=4\times10^4$	$\eta=10^5$
0.1g	5.569	5.57	5.51	5.49	5.42	5.24
0.2g	11.15	11.13	10.81	10.6	10.18	9.47
0.3g	16.76	16.73	15.80	15.17	14.36	12.94
0.4g	22.32	22.31	20.38	19.37	18.1	16.11
0.5g	27.94	27.82	24.71	23.1	21.2	18.52

4 Shaking Table Test Verification

The seismic wave used in the test is consistent with the seismic wave used in theoretical analysis. In the test, strain gauge is arranged at the root of post insulator, which is converted into stress response through elastic modulus, so as to judge the safety of structural strength; accelerometer is arranged at the flange of each sleeve to analyze the dynamic characteristics of equipment, and the sensor arrangement is shown in Fig. 20. The main test conditions are: white noise condition, frequency of test equipment; 0.2g, 0.4g seismic test condition; 0.6g shock absorption test condition; 0.8g shock absorption test condition.

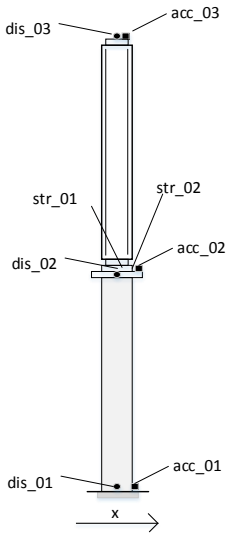

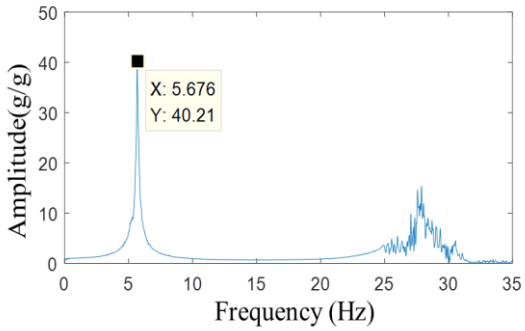

Fig. 20-Sensor layout Fig. 21-Transfer function curve of equipment under white noise

Based on the nonlinear theory, the basic frequency of the seismic model of 110kV post insulator equipment is 5.47Hz, which is smaller than the 5.68Hz obtained from the test, and the error is 10.14% respectively. Fig. 21 shows the transfer function curve of equipment under white noise condition.

Fig. 22 shows the stress time history curve of the bottom end of the porcelain pillar obtained by theory and test when the seismic excitation of the equipment is 0.2g. It can be found that the theoretical calculation results are basically consistent with the experimental results. The maximum stress of the equipment obtained from the test and theoretical analysis is 9.1MPa and 10.11MPa respectively, and the maximum stress difference is only 11%, which verifies the correctness of the seismic model.

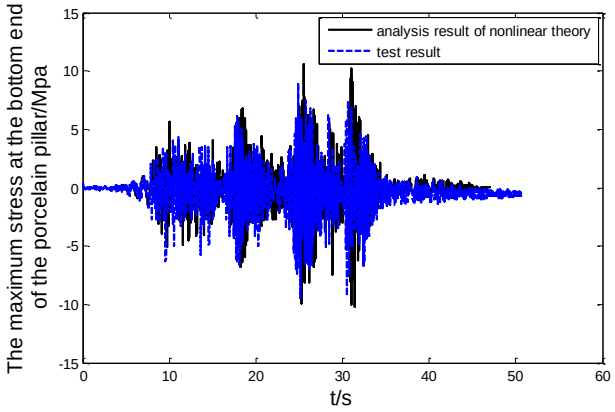

Fig. 22-The maximum stress at the bottom end of the porcelain pillar (f = 0.2g)

5 Conclusion

（1）The proposed dynamic model based on the nonlinear characteristics of the flange connection has a small error with the test results. It is proved that the theoretical model is correct when considering the nonlinear characteristics of the flanged joint. The nonlinear stiffness coefficient 20000 can represent the nonlinear characteristics of the flange connection.

（2）The nonlinear calculation results of the top displacement of the porcelain pillar and the stress at the bottom end of the porcelain pillar are smaller than the linear calculation results. With the increase of

the seismic excitation, the difference between the two increases gradually, and the nonlinear characteristics are more obvious. When the seismic excitation is 0.5g, the displacement and stress difference are 2% and 17.4% respectively.

（3） Under the excitation of each seismic wave, when the nonlinear stiffness coefficient changes within 0-10^5, the maximum stress at the bottom end of the porcelain pillar is divided into three stages: basically no change, steady decline, and rapid decline. With the nonlinear stiffness $\eta=2\times10^4$, when the seismic excitation is 0.2g, 0.3g, 0.4g, 0.5g, the maximum stress at the bottom end of the porcelain pillar is reduced by 5%, 9.5%, 13%, 17%, respectively ; With the nonlinear stiffness $\eta=4\times104$, when the seismic excitation is 0.2g, 0.3g, 0.4g, 0.5g, the maximum stress at the bottom end of the porcelain pillar is 8.7%, 14.3%, 19%, 24%, respectively. The research conclusions can provide a theoretical reference for the pillar electrical equipment.

6. Acknowledgements

This study is funded by Science and Technology Project of State Grid Corporation of China: Research on Seismic Technology of UHV Transformers based on Soil-Structure Dynamic Interaction (Grant No: 521104180015).

7. Copyrights

8. References

[1] Li S, Tsang H H, Cheng Y, et al (2016): Effects of sheds and cemented joints on seismic modelling of cylindrical porcelain electrical equipment in substations. Earthquakes and Structures, 12(1):55-65.

[2]Paolacci F, Giannini, R (2009): Seismic reliability assessment of a high-voltage disconnect switch using an effective fragility analysis. Journal of Earthquake engineering,13(2),217-235.

[3]Zhang X S, Dai Z B, Lu Z C, et al (2014): Parameter of bending stiffness of interconnected parts between ultra-high voltage porcelain bushings and flanges. Engineering Journal of Wuhan University,47(6), 794-799,858（in Chinese）

[4]Gilani. A.S, Whittaker， A.S, Fenves， G L, et al (1999): Seismic evaluation of 550kV porcelain transformer bearings. PEER Report.

[5] Whittaker，A.S, Fenves，G L, Gilani. A.S (2004): Earthquake performance of porcelain transformer bushings. Earthquake Spectra , 20(1),205-223.

[6] JEAG5003-1980,Guidelines for seismic the design of electrical equipment in substation.

[7] GB50260-2013, Code for design of seismic of electrical installations, Beijing.

